**Title page**

# A critical role for MSR1 in vesicular stomatitis virus infection of the central nervous system

Duomeng Yang[1], Tao Lin[1], Andrew G. Harrison[1], Tingting Geng[1], Huadong Wang[2], Penghua Wang[1*]

[1] Department of Immunology, School of Medicine, University of Connecticut Health Center, Farmington, CT 06030, USA

[2] Department of Pathophysiology, Key Laboratory of State Administration of Traditional Chinese Medicine of the People's Republic of China, School of Medicine, Jinan University, Guangzhou 510632, Guangdong, China

*Address correspondence to: Penghua Wang, Ph.D., Department of Immunology, School of Medicine, University of Connecticut Health Center, Farmington, CT 06030, USA. Email: pewang@uchc.edu, Tel: 860-679-6393

Running title: MSR1 is a cellular receptor for VSV

**Abstract**

Macrophage scavenger receptor 1 (MSR1) plays an important role in host defense to bacterial infections, M2 macrophage polarization and lipid homeostasis. However, its physiological function in viral pathogenesis remains poorly defined. Herein, we report that MSR1 facilitates vesicular stomatitis virus (VSV) infection in the spinal cord. Msr1-deficient (*Msr1*$^{-/-}$) mice presented reduced morbidity and mortality following lethal VSV infection, along with normal viremia and antiviral innate immune responses, compared to *Msr1*$^{+/-}$ littermates and wild-type mice. Msr1 expression was selectively upregulated in the spinal cord, which was the predominant target of VSV infection. The viral load in the spinal cord was positively correlated with Msr1 expression level and was reduced in *Msr1*$^{-/-}$ mice. Through its extracellular domain, MSR1 interacted with VSV surface glycoprotein and facilitated its cellular entry. In conclusion, our results demonstrate that MSR1 serves as a cellular entry receptor for VSV and facilitates its infection specifically in the spinal cord.

**Key words**: vesicular stomatitis virus, MSR1, scavenger receptor.

**Author Summary**

As a member of Class A scavenger receptors, macrophage scavenger receptor 1 (MSR1), recognizes various ligands including oxidized low-density lipoproteins (oxLDL), viruses and bacterial lipopolysaccharide (LPS), therefore performs many functions in tissue homeostasis and innate immunity, including pathogen clearance, lipid metabolism, macrophage polarization, and pro- or anti-inflammatory responses in different disease conditions. However, the physiological function of MSR1 during viral infection remains poorly understood. Vesicular stomatitis virus (VSV) is a negative-sense, single-stranded RNA virus, which is common in livestock (e.g. cattle, horses and swine) and produces significant economic losses. VSV is also widely used as an important model virus for fundamental research and vaccine development. But, the mechanism underlying VSV neurotropism is largely unknown. We herein report that MSR1 serves as a cellular receptor facilitating VSV infection specifically in the central nervous system. We demonstrated that MSR1 interacted with VSV virions through its extracellular domain binding to VSV-G protein, and overexpression of the extracellular domain alone was sufficient to promote VSV infection. Our results reveal a novel function for Msr1 as a critical determinant of VSV infection specifically in the spinal cord.

## Introduction

Macrophage scavenger receptor 1 (MSR1; also known as CD204, SCARA1 and SR-A1), a member of Class A scavenger receptors, performs many functions in homeostasis and immunity, including pathogen clearance, lipid metabolism and macrophage polarization [1]. MSR1 recognizes a wide range of ligands including oxidized low-density lipoprotein (oxLDL), endogenous proteins, beta-amyloid, lipoteichoic acid (LTA) and bacterial lipopolysaccharide (LPS) [2, 3]. The ligand promiscuity of MSR1 is probably due to its function as a component of other pathogen pattern recognition receptor (PRR) signaling complexes. For instance, MSR1 interacts with receptor tyrosine kinase MER (MERTK) to enable apoptotic cell clearance [4]. MSR1 partners with TLR4 to sense LPS that leads to activation of nuclear factor-κB (NF-κB) signaling [5], and therefore contributes to either a pro- or anti-inflammatory responses in Alzheimer's disease, sepsis, cancer and atherosclerosis conditions [6-8]. MSR1 recognizes and internalizes dead cells or debris through interaction with spectrin in macrophages [9]. MSR1 also promotes M2 macrophage polarization and Th2 cell responses to bacterial infection by suppressing nuclear translocation of interferon regulatory factor 5 (IRF5) [10]. The functions of MSR1 during viral infection may vary with virus species and disease conditions. MSR1 signaling may protect mice against lethal herpes simplex virus infection [11], activate autophagy to control Chikungunya virus infection [12] and limit replication-defective adenovirus type 5-elicited hepatic inflammation and fibrosis by promoting M2 macrophage polarization [13]. MSR1 appears to function as a carrier of extracellular dsRNA of hepatitis C virus and present it to endosomal TLR3 and cytoplasmic RIG-I like receptors, resulting in an antiviral type I IFN response [14,

86 15]. However, MSR1 signaling could aggravate the pathogenesis of murine hepatitis
87 virus-induced fulminant hepatitis by enhancing neutrophil NETosis formation-induced
88 complement activation [16].

89 Vesicular stomatitis virus (VSV) is a negative-sense, single-stranded RNA virus of the
90 *Rhabdoviridae* family. This bullet-shaped virus infects a wide range of cells through its
91 surface glycoprotein (VSV-G) [17, 18]. Although VSV infection in humans is rare and very
92 mild, it is common in livestock (e.g. cattle, horses and swine) and may produce significant
93 economic losses, particularly in the southwestern states of the Unites States [19]. Because of
94 its broad cell tropism, easily genetic engineering and lack of preexisting human immunity
95 against it, VSV is widely used as a model virus for fundamental research and vaccine
96 development [20, 21]. Like rabies virus, VSV is a neurotropic virus that primarily infects
97 animals and occasionally humans [22-24]. However, the mechanisms underlying VSV
98 neurotropism remains unclear. Herein, we report that Msr1 facilitates VSV infection in the
99 spinal cord specifically. Msr1 serves as a cellular receptor that is selectively and highly
100 upregulated in the spinal cord following VSV infection. Msr1-deficiency thus renders mice
101 resistant to lethal VSV infection.

102

103 **Results**

104 **Msr1 contributes to VSV pathogenesis in mice**

105 MSR1 plays an important role in host defense to microbial infections [1]. However, its
106 physiological function in viral pathogenesis may vary significantly with viral species. We
107 investigate this using VSV, a model RNA virus for the study of innate antiviral immune

108 responses. Msr1 mRNA was expressed in various tissues with the highest in spleen (Fig. 1a).
109 We then infected *Msr1*$^{-/-}$ and wild-type (WT, C57BL/6) control mice with a lethal dose of
110 VSV. Intriguingly, ~90% of the WT mice (n=12) succumbed to VSV infection, but only ~30%
111 *Msr1*$^{-/-}$ mice died (n=12) (Fig. 1b). The overall survival rate of *Msr1*$^{-/-}$ mice was much higher
112 than that of WT mice ($P$=0.001, Log-Rank test). In addition, the disease severity of WT mice
113 was continuously increased from day 4 after infection and much greater than *Msr1*$^{-/-}$ mice
114 (Fig. 1b). Almost all infected WT mice developed severe symptoms such as hind-limb
115 paralysis as well as decreased mobility (Fig. 1c). To validate the phenotypic results, we
116 produced *Msr1*$^{-/-}$ and *Msr1*$^{-/+}$ littermates and repeated VSV infection. We confirmed that
117 Msr1 protein level in *Msr1*$^{+/-}$ was the same as that in WT macrophages, which express
118 abundant Msr1 (Fig. 1d). Consistently, the survival rate and disease score of *Msr1*$^{+/-}$ mice
119 infected with VSV were similar with WT mice. ~ 80% of infected *Msr1*$^{+/-}$ mice (n=6)
120 presented severe hind-limb paralysis and succumbed to lethal VSV infection, while none of
121 *Msr1*$^{-/-}$ mice (n=6) showed severe symptoms (Fig. 1e). These data suggest that Msr1
122 contributes to the pathogenesis of VSV-induced disease.

123 Msr1 plays an important role in the maintenance of immune homeostasis and is reported
124 to aggravate virus-induced fulminate hepatitis pathogenesis by mediating C5a-induced
125 proinflammatory response[16]. We thus assessed VSV viremia and the serum levels of type I
126 IFN and inflammatory cytokines between VSV-infected WT, *Msr1*$^{+/-}$ and *Msr1*$^{-/-}$ littermates
127 by multiplex ELISA and quantitative RT-PCR. Interestingly, the viremia and cytokine levels
128 (i.e. IFN-α, IFN-γ, TNF-α, IL-10, CXCL-10, IL-1β) in *Msr1*$^{-/-}$ mice were similar to WT and
129 *Msr1*$^{+/-}$ littermates (Fig. 2a, b, Fig. S1a, b). These results demonstrate that Msr1 is

130 dispensable for systemic VSV dissemination and innate immune responses.

131 **Msr1 is critical for VSV infection in the spinal cord**

132 VSV shows a strong neurotropism and causes severe neurological disorders in a variety of
133 rodent and primate animals though the underlying mechanism remains elusive [25]. Indeed,
134 we observed overt hind-limb paralysis and immobility in WT mice (Fig. 1b-e), indicative of
135 severe infection in the central nervous system (CNS). We therefore evaluated viral loads in
136 different tissues after VSV infection. As shown in Fig. 3a, the VSV load in the spinal cord
137 was much higher than other tissues in VSV-infected *Msr1*$^{+/-}$ mice. Then, we examined the
138 CNS specimens from VSV-infected *Msr1*$^{+/-}$ and *Msr1*$^{-/-}$ littermates. We found that the viral
139 load in the spinal cord of *Msr1*$^{-/-}$ mice was significantly lower than that of *Msr1*$^{+/-}$ mice, while
140 the difference in the brain was moderate (Fig. 3b-d). This result is consistent with
141 VSV-induced severe paraplegia, which is most often caused by spinal cord injury [26].
142 Interestingly, the *Msr1* expression was sharply induced by VSV in the spinal cord and
143 modestly in the liver, while decreased in the spleen after infection (Fig. 3e). A strong positive
144 correlation between *Msr1* expression level and VSV load in the spinal cord was noted; the
145 association was moderate in the brain and spleen (Fig. 3f), suggesting that Msr1 is a
146 determinant of VSV infection in the spinal cord.

147 The scavenger receptor family consists of 10 classes, which are structurally
148 heterogeneous with little or no homology [1]. MSR1 belongs to the Class A receptors, which
149 all have a extracellular collagenous domain [1]. The aforementioned results suggest that
150 MSR1 is upregulated by VSV specifically in the spinal cord. We then asked if other members
151 of Class A and B may be induced similarly by VSV. The results show that *CD36* (*Scarb3*)

152 was also markedly induced in the spinal cord after VSV infection (Fig. 3g), but none of the
153 Class A/B scavenger receptors tested were significantly changed in the expression levels in
154 the infected brain (Fig. 3h). The LDL receptor family members serve as the cellular receptors
155 for VSV [27], and are also expressed in the nervous system [28]; we thus examined the
156 expression of *Ldlr* in the brain and spinal cord. Intriguingly, *Ldlr* expression was higher in
157 the spinal cord than brain, but not significantly changed after VSV infection in either tissue
158 (Fig. 3i). These findings suggest that Msr1 is critical for VSV infection, specifically in the
159 spinal cord.
160

161 **Msr1 mediates cellular entry of VSV**

162 The above-mentioned data suggest that MSR1 may facilitate VSV infection directly. Of note,
163 MSR1 is known to recognize a wide range of self- and microbial ligands, in particular,
164 oxidized low density lipoproteins[2, 3]. We thus hypothesized that MSR1 could mediate
165 cellular entry of VSV. To this end, we employed primary neuron culturing from neonatal
166 *Msr1*$^{+/-}$ and *Msr1*$^{-/-}$ littermates and bone marrow-derived macrophages (BMDM) which
167 express abundant Msr1 (Fig. 4c). Indeed, the VSV load in *Msr1*$^{-/-}$ neurons (Fig. 4a) and the
168 virus titer in its culture medium (Fig. 4b) were significantly decreased compared to *Msr1*$^{+/-}$
169 littermates. The intracellular VSV-G protein level and extracellular infectious virions in
170 *Msr1*$^{-/-}$ BMDMs were much lower than those in WT cells (Fig. 4d-f). We next determined if
171 cellular entry of VSV was impaired in *Msr1*$^{-/-}$ cells. BMDMs were inoculated with VSV at 4 ℃
172 for 2hrs to allow for VSV attachment to the cell surface, at 37 ℃ for 30 min to allow for VSV
173 entry into cells, and lastly were washed extensively to remove unbound virions. Indeed, there

174 were fewer VSV virions attached to *Msr1*$^{-/-}$ than WT cells at 4 ℃ and consequently fewer
175 virions inside *Msr1*$^{-/-}$ cells at 37 ℃ (Fig. 4g). These data show that Msr1 mediates cellular
176 entry of VSV.

177 Human MSR1 protein shares 70% identity and 81% similarity with mouse Msr1. We
178 then asked if the function of MSR1during VSV infection is evolutionarily conserved. To this
179 end, we evaluated VSV infection in a human *MSR1*$^{-/-}$ trophoblast line that was generated
180 recently in our hands [12]. Indeed, VSV-G protein level in *MSR1*$^{-/-}$ trophoblasts was much
181 less than that in WT cells at 12 hrs after VSV infection (Fig. 5a). Consistently, the
182 fluorescence intensity of VSV-GFP in *MSR1*$^{-/-}$ trophoblasts was also decreased compared to
183 WT cells (Fig. 5b), and the plaque assay further showed a significant reduction in VSV
184 virions in the culture medium of *MSR1*$^{-/-}$ compared to WT trophoblasts (Fig. 5c).
185 Overexpression of MSR1 significantly increased VSV-G protein level (Fig. 5d), VSV-GFP
186 fluorescence intensity (Fig. 5e), and VSV titer in the cell culture medium (Fig. 5f), compared
187 to the vector control. Epichromosomal complementation of MSR1 gene in *MSR1*$^{-/-}$
188 trophoblasts restored VSV infection (Fig. 5g).

189 MSR1 is a cell surface protein with a short intracellular N-terminus, a transmembrane
190 domain and a long extracellular portion. We postulated that the extracellular portion mediates
191 VSV entry. To prove this, we dissected MSR1 into several fragments: amino residues 1-50
192 (cytoplasmic N-tail), 1-80 (cytoplasmic N-tail plus transmembrane), and 51-end
193 (extracellular domains with transmembrane), expressed them in trophoblasts (Fig. 5h, Fig.
194 S2a) and infected cells with VSV-GFP for 12 hrs. Intriguingly, both the fragment (51-end)
195 and full-length (1-end) MSR1 enhanced VSV-G protein level and VSV-GFP fluorescence

196 intensity; while the fragments without the extracellular domains (1-50 and 1-80) failed to do
197 so (Fig. 6i, j). These results demonstrate that MSR1 facilitates cellular entry of VSV through
198 its extracellular domain.

199 **MSR1 interacts with VSV glycoprotein G via its extracellular domain**

200 Based on the aforementioned data, we hypothesized that MSR1 serves as a cellular receptor
201 for VSV. We thus employed an immunoprecipitation assay to investigate if MSR1 full-length
202 (1-end) and/or fragments (1-80, 51-end, respectively) directly interact with intact VSV-GFP
203 virions. In agreement with Fig. 5h-j, both the 51-end and full-length of MSR1 pulled-down
204 infectious virions; while the MSR1 (1-80) did not (Fig. 6a-c). Of note, with considerably less
205 protein expression, the 51-end fragment pulled down the same amount of VSV-GFP as
206 full-length MSR1 (Fig. 6a-c), suggesting that the extracellular fragment mediates MSR1
207 binding to VSV virions. We further asked if MSR1 directly interacts with VSV surface
208 glycoprotein G that mediates VSV entry into host cells. We performed co-transfection of
209 VSV-G and FLAG-MSR1/fragment plasmids into HEK293 cells and immunoprecipitation
210 using an anti-FLAG antibody. The results show that the fragment (51-end) and full-length
211 (1-end) FLAG-MSR1 pulled down VSV-G, while the empty vector and the fragment 1-80 did
212 not (Fig. 6d).

213

214 **Discussion**

215 Although MSR1 has proven to perform a variety of functions in homeostasis and host
216 immunity due to its ability to recognize a diverse range of ligands [2, 3], its role in viral
217 pathogenesis remains poorly defined. MSR1 signaling may be protective against

218 Chikungunya virus and herpes simplex virus infection [11, 12], but could also contribute to
219 hepatitis virus-induced liver damage [16]. In this study, our data collectively demonstrate that
220 MSR1 serves as a cellular receptor facilitating VSV infection specifically in the spinal cord,
221 and this is substantiated by several lines of experimental evidence. Firstly, Msr1-deficient
222 mice were strikingly resistant to VSV-elicited hind-limb paralysis compared to their
223 wild-type littermates. However, Msr1 was dispensable for systemic VSV dissemination and
224 innate immune responses. Secondly, the viral load in the spinal cord was the highest and the
225 fold induction of Msr1 expression by VSV was the greatest among all tested tissues. Of note,
226 the Msr1 expression level was positively correlated with VSV load in the spinal cord. These
227 results not only demonstrate a strong tropism of VSV for the spinal cord that leads to severe
228 paraplegia[26],[25], but also reveal a novel function for Msr1 as a critical determinant of
229 VSV infection specifically in the spinal cord. Thirdly, VSV attachment, entry, and
230 consequently replication was significantly reduced in both mouse primary *Msr1*$^{-/-}$
231 macrophages and human *MSR1*$^{-/-}$ trophoblasts. While overexpression of MSR1 could enhance
232 cellular entry of VSV and subsequent replication. Lastly, MSR1, through its extracellular
233 domain, interacted with VSV virions through its surface glycoprotein G and overexpression
234 of the extracellular section alone was sufficient to promote VSV infection. These
235 observations suggest that MSR1 is an entry receptor for VSV [17, 18].

236 To date, the membrane lipid phosphatidylserine and endoplasmic reticulum chaperone
237 Gp96 are important for VSV entry, but not as a receptor [25]. The LDL receptor and its
238 family members were recently characterized as entry receptors for VSV in both human and
239 mouse cells [27]. The widespread expression pattern of the LDLR family members may thus

240 in part underlie VSV pantropism. However, the *Rhabdoviridae* viruses (e.g. rabies virus,
241 VSV) specifically invade and replicate in motor neurons that exist predominately in the
242 spinal cord [29], and subsequent retrograde or anterograde spread of progeny virions in the
243 motor nerve system results in paraplegia [30, 31]. Indeed, this study demonstrates that VSV
244 primarily targets the spinal cord, and secondarily the brain. Intriguingly MSR1 is essential for
245 VSV infection only in the spinal cord. In agreement with this, among all tested Class A and B
246 scavenger receptors, MSR1 is the most significantly upregulated member in the spinal cord;
247 while LDLR expression is unchanged following VSV infection. These observations suggest
248 that MSR1 becomes important for VSV infection of the spinal cord at least partly because
249 MSR1 expression is robustly upregulated. On the other hand, MSR1 could contribute to
250 neuronal inflammation and apoptosis by activating NF-κB signaling pathway in the spinal
251 cord [32]. However, our data do not necessarily rule out the importance of LDLR family to
252 VSV infection in the spinal cord. Indeed, LDLR expression in the spinal cord, either before
253 or after VSV infection, is much higher than the brain.

254 In sum, we herein define MSR1 as a cellular entry receptor for VSV infection
255 specifically in the spinal cord. MSR1 can be selectively and highly upregulated in the spinal
256 cord following VSV infection. Given that VSV and its pseudotyped viruses have been widely
257 applied to vaccine research and oncolytic therapy [33-35], it seems plausible to improve
258 VSV-mediated oncolytic efficacy by manipulating MSR1 expression.

259

260

261 **Materials and Methods**

262 *Animals*

263 All mice were purchased from the Jackson Laboratory and housed under the same conditions.
264 C57BL/6J mice (Stock No: 000664) were employed as the wild-type control mice. *Msr1*$^{-/-}$
265 mice (B6.Cg-*Msr1*$^{tm1Csk}$/J, stock No: 006096) were made from 129 embryonic stem (ES) cells
266 and then backcrossed to C57BL/6J mice for 12 generations. *Msr1*$^{+/-}$ mice were made by
267 backcrossing *Msr1*$^{-/-}$ mice to C57BL/6J mice. All of the gene-mutant and wild type mice
268 were normal in body weight and general health. Sex- and age-matched (6-8 weeks) mice
269 were used for all the experiments. The animal protocols were approved by the Institutional
270 Animal Care & Use Committee at University of Connecticut adhering to the National
271 institutes of Health recommendations for the care and use of laboratory animals.

272

273 *Antibodies and plasmids*

274 The rabbit anti-Actin (Cat # 8456) antibody was purchased from Cell Signaling Technology
275 (Danvers, MA 01923, USA). The mouse anti-FLAG (Cat# TA50011) and rabbit
276 anti-human/mouse MSR1 (Cat# TA336699) antibodies were from Origene (Rockville, MD
277 20850, USA). The mouse anti-human MSR1 (Cat# MAB2708) antibody was obtained from
278 R&D Systems (Minneapolis, MN 55413, USA). Then rabbit anti-VSV-G (Cat#V4888)
279 antibody and the anti-FLAG M2 magnetic beads (Clone M2, Cat# M8823) were from
280 Sigma-Aldrich (St. Louis, MO, USA). The human MSR1 (Cat# RC209609) were obtained
281 from Origene (Rockville, MD 20850, USA). Human MSR1 and its fragment 1-50, 1-80 and
282 51-end were amplified by PCR and inserted into pcDNA3.1 (Zeo)-FLAG vector. The primers

283 are listed in the Supplemental Table S1.

284

285 *Cell culture and viruses*

286 Vero cells (monkey kidney epithelial cells, # CCL-81), human trophoblasts HTR-8/SVneo
287 (#CRL-3271) and L929 (mouse fibroblast cells, # CCL-1) were purchased from American
288 Type Culture Collection (ATCC) (Manassas, VA20110, USA). *MSR1*$^{-/-}$ trophoblasts were
289 generated in our previous study [12]. Vero cells were grown in Corning® DMEM
290 (Dulbecco's Modified Eagle's Medium) supplemented with 10% FBS and 1%
291 penicillin/streptomycin. Human trophoblasts were cultured in Corning® RPMI 1640 medium
292 supplemented with 10% fetal bovine serum and 1% penicillin/streptomycin. Bone
293 marrow-derived macrophages (BMDMs) were differentiated from femur bone-derived bone
294 marrows in L929 conditioned medium (RPMI1640, 20%FBS, 30% L929 culture medium and
295 1% penicillin/streptomycin) in 10-cm Petri-dishes at 37 °C, 5% $CO_2$ for 7 days. The BMDMs
296 were then seeded in culture plates and cultured in regular RPMI1640 medium overnight
297 before further treatment. MycoZap (Lonza) were used regularly to prevent mycoplasma
298 contamination. The vesicular stomatitis virus (VSV) used in this study was Indiana strain
299 described previously [36], and the green fluorescence protein (GFP) tagged VSV was made
300 from this VSV. These viruses were propagated in Vero cells.

301

302 *Primary neuron culture*

303 The primary neuron culturing was performed according to a previous method[37]. The brain
304 of a 3-day old neonate was dissected dorsally under a microscope; the vascular tunic was

305 removed; and then the brain was washed in ice-cold DMEM medium. The brain was then
306 broken into pieces by pipetting up and down in 0.125% trypsin with DNAse I, and then
307 digested for 30min in a 37 °C water bath, vortexed every 10 min. Digestion of the brain was
308 terminated by 10% FBS+DMEM, filtered through a 70μm cell strainer (ThemoFisher brand).
309 The filtrate was centrifuged at 500 x g at 4 °C for 5min to pellet neurons. The neurons were
310 then plated in 0.0125% poly-L-lysine-coated culture plates (overnight at 37°C), and cultured
311 in neurobasal medium (Gibco, U.S) with 2% B27 supplement (Gibco, U.S) at 37 °C, 5% $CO_2$
312 for 5-6 days.
313
314 *Mouse infection and disease monitoring*
315 VSV stock [~$10^8$ plaque forming units (PFU/ml)] was diluted in sterile phosphate buffered
316 saline (PBS), and ~$10^7$ PFU was injected into mice retro-orbitally [38]. The mice were
317 monitored for disease progression over a period of 8 days after infection. The main symptoms
318 were mobility and hind-limb paralysis. The severity of disease was measured using a scale
319 from 0 (no symptom), 1 (no plantar stepping in one hind leg), 2 (no plantar stepping in two
320 hind legs or slight ankle movement in one hind leg), 3 (slight ankle movement in two hind
321 legs or no ankle movement in one hind leg), 4 (no ankle movement in one hind leg and slight
322 in the other one) to 5 (no ankle movement in both hind legs, almost loss of all movement
323 ability), as described previously [26]. The mice scored for 5 were euthanized as a humane
324 endpoint according to the animal protocol.
325
326 *Real-time reverse transcription PCR*

327 Animal tissues or whole blood (30µl) were collected in 330µl of lysis buffer (Invitrogen
328 RNAasy mini-prep kit). The heart, liver, lung, brain and spleen were minced with a pair of
329 scissors and homogenized in RLT buffer using an electrical pellet pestle (Kimble Chase LLC,
330 USA). RNA was extracted following the Invitrogen RNAasy mini-prep kit protocol, and
331 reverse-transcribed into cDNA using the TAKARA PrimeScriptTM RT Reagent Kit with
332 gDNA Eraser (Perfect Real Time) (#RR047A). qPCR was performed with gene-specific
333 primers and Bio-Rad SYBR Premix. qPCR results were calculated using the –ΔΔCt method
334 and beta actin gene as an internal control. The qPCR primers are summarized in supplemental
335 material Table S2.
336
337 *Plaque-forming assay*
338 The viral particles in tissue homogenates or cell culture medium were quantitated by plaque
339 forming assays as previously described [39]. Briefly, samples were serially diluted by 10-fold
340 using DMEM without FBS, and then 500 µL of each diluted sample plus 500 µL DMEM
341 without FBS were added onto a Vero cell monolayer in a 6-well plate. The 6-well plate was
342 then incubated at 37 °C for 2 h. The inoculum was replaced with 1% SeaPlaque agarose (Cat#
343 50100, Lonza) in complete DMEM medium (2 ml). The plate was left at room temperature
344 for 30min to allow the agarose to solidify, and then moved to a cell culture incubator (37 °C,
345 5% $CO_2$). Plaques were visualized by a Neutral Red exclusion assay after 3 days.
346
347 *Western blotting assay*
348 Western blotting analysis was performed using standard procedures. Briefly, protein samples

349 were resolved by SDS-PAGE (sodium dodecyl sulfate-polyacrylamide gel electrophoresis)
350 and transferred to a nitrocellulose membrane. The membrane blot was incubated with a
351 primary antibody over night at 4 ℃, washed briefly and incubated with a HRP-conjugated
352 secondary antibody for 1 hour at room temperature. An ultra-sensitive ECL substrate was
353 used for detection (ThermoFisher, Cat# 34095).
354
355 *Co-immunoprecipitation*
356 Trophoblasts or HEK293 cells were seeded at a density of $5x10^5$ cells/ml and transfected with
357 protein expression plasmids (pVSVG, 1-80, 51-end, 1-end of FLAG-MSR1, and vector)
358 using TransIT-X2® Transfection Reagent. Twenty-four hours after transfection, whole-cell
359 extracts were prepared from transfected trophoblasts in lysis buffer (150 mM NaCl, 50 mM
360 Tris pH 7.5, 1 mM EDTA, 0.5% NP40, 10% Glycerol) and were incubated with 50µl of
361 anti-FLAG magnetic beads for 2hrs at 4°C. The whole procedure of co-immunoprecipitation
362 was performed according to manufacturer's protocol (Anti-Flag Magnetic Beads,
363 Sigma-Aldrich). For co-immunoprecipitation of live VSV particles, $5x10^5$ cells/ml HEK293
364 cells were transfected with protein expression plasmids (1-80, 51-end, 1-end of FLAG-MSR1,
365 and vector). Twenty-four hours later, cells were lysed in lysis buffer and incubated with 50µl
366 of anti-FLAG magnetic beads for 2hrs at 4°C. The beads were washed three times with sterile
367 PBS to completely remove detergent and unbound cellular proteins, and were then incubated
368 with VSV-GFP virions (500µl, $1x10^7$ PFU/ml) for 2hrs at 4°C. The beads were washed with
369 sterile PBS three times to remove unbound virions and the bound virions were eluted with
370 3xFLAG peptide in sterile PBS. The VSV-GFP pulled down by FLAG-MSR1 and fragments

371 were then used to infect Vero cells or immunoblotting (Fig. S2b).

372

373 *Multiplex ELISA (enzyme-linked immunosorbent assay)*

374 BioLegend's LEGENDplex™ bead-based immunoassays of serum samples were performed
375 exactly according to the instruction of BioLegend's LEGENDplex™ kit. The flow cytometry
376 data were analyzed using the LEGENDplex™ data analysis software.

377

378 *Graphing and statistics*

379 The data from all experiments were analyzed using a Prism GraphPad Software and
380 expressed as mean ± S.D. Survival data were analyzed using a Log-rank (Mantel-Cox) test.
381 For *in vitro* cell culture results, a standard two-tailed unpaired Student's t-test was used. For
382 animal studies, an unpaired two-tailed nonparametric Mann-Whitney U test was applied to
383 statistical analysis. $P$ values $\leq 0.05$ were considered significant. The statistic statements of
384 experiments are detailed in each figure legend.

385

386

**Acknowledgements**

This work was supported by a National Institutes of Health grant R01AI132526 and UConn Health startup fund to P.W.

**Author contributions**

D.Y. designed and performed all the experimental procedures and data analyses. T.L., A.H., and T.G provided technical support and/or data analyses. H.W. assisted with data interpretation and discussion. P.W. conceived and oversaw the study. D.Y. and P.W. wrote the paper and all the authors reviewed and/or modified the manuscript.

**Conflict of interest**

The authors declare no competing financial/non-financial interest.

401 **References**


402 1. Canton J, Neculai D, Grinstein S. Scavenger receptors in homeostasis and immunity. Nature reviews
403 Immunology. 2013;13(9):621-34. doi: 10.1038/nri3515. PubMed PMID: 23928573.
404 2. Pluddemann A, Mukhopadhyay S, Gordon S. Innate immunity to intracellular pathogens: macrophage
405 receptors and responses to microbial entry. Immunological reviews. 2011;240(1):11-24. Epub 2011/02/26. doi:
406 10.1111/j.1600-065X.2010.00989.x. PubMed PMID: 21349083.
407 3. Pombinho R, Sousa S, Cabanes D. Scavenger Receptors: Promiscuous Players during Microbial
408 Pathogenesis. Critical reviews in microbiology. 2018;44(6):685-700. Epub 2018/10/16. doi:
409 10.1080/1040841X.2018.1493716. PubMed PMID: 30318962.
410 4. Todt JC, Hu B, Curtis JL. The scavenger receptor SR-A I/II (CD204) signals via the receptor tyrosine kinase
411 Mertk during apoptotic cell uptake by murine macrophages. Journal of leukocyte biology. 2008;84(2):510-8.
412 Epub 2008/05/31. doi: 10.1189/jlb.0307135. PubMed PMID: 18511575; PubMed Central PMCID:
413 PMCPmc2718803.
414 5. Yu H, Ha T, Liu L, Wang X, Gao M, Kelley J, et al. Scavenger receptor A (SR-A) is required for LPS-induced
415 TLR4 mediated NF-kappaB activation in macrophages. Biochimica et biophysica acta. 2012;1823(7):1192-8.
416 Epub 2012/05/26. doi: 10.1016/j.bbamcr.2012.05.004. PubMed PMID: 22627090; PubMed Central PMCID:
417 PMCPmc3382073.
418 6. Kelley JL, Ozment TR, Li C, Schweitzer JB, Williams DL. Scavenger receptor-A (CD204): a two-edged sword
419 in health and disease. Critical reviews in immunology. 2014;34(3):241-61. Epub 2014/06/19. doi:
420 10.1615/critrevimmunol.2014010267. PubMed PMID: 24941076; PubMed Central PMCID: PMCPmc4191651.
421 7. Zhang Y, Wei Y, Jiang B, Chen L, Bai H, Zhu X, et al. Scavenger Receptor A1 Prevents Metastasis of
422 Non–Small Cell Lung Cancer via Suppression of Macrophage Serum Amyloid A1. Cancer Research.
423 2017;77(7):1586. doi: 10.1158/0008-5472.CAN-16-1569.
424 8. Mukhopadhyay S, Varin A, Chen Y, Liu B, Tryggvason K, Gordon S. SR-A/MARCO-mediated ligand delivery
425 enhances intracellular TLR and NLR function, but ligand scavenging from cell surface limits TLR4 response to
426 pathogens. Blood. 2011;117(4):1319-28. Epub 2010/11/26. doi: 10.1182/blood-2010-03-276733. PubMed
427 PMID: 21098741.
428 9. Cheng C, Hu Z, Cao L, Peng C, He Y. The scavenger receptor SCARA1 (CD204) recognizes dead cells
429 through spectrin. The Journal of biological chemistry. 2019;294(49):18881-97. Epub 2019/10/28. doi:
430 10.1074/jbc.RA119.010110. PubMed PMID: 31653705; PubMed Central PMCID: PMCPmc6901321.
431 10. Xu Z, Xu L, Li W, Jin X, Song X, Chen X, et al. Innate scavenger receptor-A regulates adaptive T helper cell
432 responses to pathogen infection. Nature communications. 2017;8:16035. Epub 2017/07/12. doi:
433 10.1038/ncomms16035. PubMed PMID: 28695899; PubMed Central PMCID: PMCPmc5508227.
434 11. Suzuki H, Kurihara Y, Takeya M, Kamada N, Kataoka M, Jishage K, et al. A role for macrophage scavenger
435 receptors in atherosclerosis and susceptibility to infection. Nature. 1997;386(6622):292-6. doi:
436 10.1038/386292a0. PubMed PMID: 9069289.
437 12. Yang L, Geng T, Yang G, Ma J, Wang L, Ketkhar H, et al. Macrophage scavenger receptor 1 controls
438 Chikungunya virus infection through autophagy. bioRxiv. 2020:2020.02.28.969832. doi:
439 10.1101/2020.02.28.969832.
440 13. Labonte AC, Sung S-SJ, Jennelle LT, Dandekar AP, Hahn YS. Expression of scavenger receptor-AI promotes
441 alternative activation of murine macrophages to limit hepatic inflammation and fibrosis. Hepatology.
442 2017;65(1):32-43. Epub 11/22. doi: 10.1002/hep.28873. PubMed PMID: 27770558.
443 14. DeWitte-Orr SJ, Collins SE, Bauer CM, Bowdish DM, Mossman KL. An accessory to the 'Trinity': SR-As are

444 essential pathogen sensors of extracellular dsRNA, mediating entry and leading to subsequent type I IFN
445 responses. PLoS pathogens. 2010;6(3):e1000829. Epub 2010/04/03. doi: 10.1371/journal.ppat.1000829.
446 PubMed PMID: 20360967; PubMed Central PMCID: PMCPmc2847946.
447 15. Dansako H, Yamane D, Welsch C, McGivern DR, Hu F, Kato N, et al. Class A scavenger receptor 1 (MSR1)
448 restricts hepatitis C virus replication by mediating toll-like receptor 3 recognition of viral RNAs produced in
449 neighboring cells. PLoS pathogens. 2013;9(5):e1003345. Epub 2013/05/30. doi: 10.1371/journal.ppat.1003345.
450 PubMed PMID: 23717201; PubMed Central PMCID: PMCPmc3662657.
451 16. Tang Y, Li H, Li J, Liu Y, Li Y, Zhou J, et al. Macrophage scavenger receptor 1 contributes to pathogenesis of
452 fulminant hepatitis via neutrophil-mediated complement activation. Journal of hepatology. 2018;68(4):733-43.
453 doi: 10.1016/j.jhep.2017.11.010. PubMed PMID: 29154963; PubMed Central PMCID: PMC5951742.
454 17. Ge P, Tsao J, Schein S, Green TJ, Luo M, Zhou ZH. Cryo-EM model of the bullet-shaped vesicular stomatitis
455 virus. Science. 2010;327(5966):689-93. Epub 2010/02/06. doi: 10.1126/science.1181766. PubMed PMID:
456 20133572; PubMed Central PMCID: PMCPmc2892700.
457 18. Nikolic J, Belot L, Raux H, Legrand P. Structural basis for the recognition of LDL-receptor family members
458 by VSV glycoprotein. Nature communications. 2018;9(1):1029. doi: 10.1038/s41467-018-03432-4. PubMed
459 PMID: 29531262.
460 19. Rozo-Lopez P, Drolet BS, Londoño-Renteria B. Vesicular Stomatitis Virus Transmission: A Comparison of
461 Incriminated Vectors. Insects. 2018;9(4):190. doi: 10.3390/insects9040190. PubMed PMID: 30544935.
462 20. Bukreyev A, Skiadopoulos MH, Murphy BR, Collins PL. Nonsegmented negative-strand viruses as vaccine
463 vectors. Journal of virology. 2006;80(21):10293-306. Epub 2006/10/17. doi: 10.1128/jvi.00919-06. PubMed
464 PMID: 17041210; PubMed Central PMCID: PMCPmc1641758.
465 21. Mátrai J, Chuah MKL, VandenDriessche T. Recent advances in lentiviral vector development and
466 applications. Mol Ther. 2010;18(3):477-90. Epub 01/19. doi: 10.1038/mt.2009.319. PubMed PMID: 20087315.
467 22. Gagnidze K, Hajdarovic KH, Moskalenko M, Karatsoreos IN, McEwen BS, Bulloch K. Nuclear receptor
468 REV-ERBalpha mediates circadian sensitivity to mortality in murine vesicular stomatitis virus-induced
469 encephalitis. Proceedings of the National Academy of Sciences of the United States of America.
470 2016;113(20):5730-5. Epub 2016/05/05. doi: 10.1073/pnas.1520489113. PubMed PMID: 27143721; PubMed
471 Central PMCID: PMCPmc4878505.
472 23. Quiroz E, Moreno N, Peralta PH, Tesh RB. A human case of encephalitis associated with vesicular
473 stomatitis virus (Indiana serotype) infection. The American journal of tropical medicine and hygiene.
474 1988;39(3):312-4. Epub 1988/09/01. doi: 10.4269/ajtmh.1988.39.312. PubMed PMID: 2845825.
475 24. Ludlow M, Kortekaas J, Herden C, Hoffmann B, Tappe D, Trebst C, et al. Neurotropic virus infections as
476 the cause of immediate and delayed neuropathology. Acta neuropathologica. 2016;131(2):159-84. Epub
477 2015/12/15. doi: 10.1007/s00401-015-1511-3. PubMed PMID: 26659576; PubMed Central PMCID:
478 PMCPmc4713712.
479 25. Hastie E, Cataldi M, Marriott I, Grdzelishvili VZ. Understanding and altering cell tropism of vesicular
480 stomatitis virus. Virus research. 2013;176(1-2):16-32. Epub 2013/06/26. doi: 10.1016/j.virusres.2013.06.003.
481 PubMed PMID: 23796410; PubMed Central PMCID: PMCPmc3865924.
482 26. Smith PD, Bell MT, Puskas F, Meng X, Cleveland JC, Jr., Weyant MJ, et al. Preservation of motor function
483 after spinal cord ischemia and reperfusion injury through microglial inhibition. The Annals of thoracic surgery.
484 2013;95(5):1647-53. Epub 2013/04/02. doi: 10.1016/j.athoracsur.2012.11.075. PubMed PMID: 23541432.
485 27. Finkelshtein D, Werman A, Novick D, Barak S, Rubinstein M. LDL receptor and its family members serve as
486 the cellular receptors for vesicular stomatitis virus. Proceedings of the National Academy of Sciences of the
487 United States of America. 2013;110(18):7306-11. Epub 2013/04/17. doi: 10.1073/pnas.1214441110. PubMed

488 PMID: 23589850; PubMed Central PMCID: PMCPmc3645523.
489 28. Beffert U, Stolt PC, Herz J. Functions of lipoprotein receptors in neurons. Journal of lipid research.
490 2004;45(3):403-9. Epub 2003/12/06. doi: 10.1194/jlr.R300017-JLR200. PubMed PMID: 14657206.
491 29. Bradbury EJ, McMahon SB. Spinal cord repair strategies: why do they work? Nature reviews Neuroscience.
492 2006;7(8):644-53. Epub 2006/07/22. doi: 10.1038/nrn1964. PubMed PMID: 16858392.
493 30. Beier KT, Saunders A, Oldenburg IA, Miyamichi K, Akhtar N, Luo L, et al. Anterograde or retrograde
494 transsynaptic labeling of CNS neurons with vesicular stomatitis virus vectors. Proceedings of the National
495 Academy of Sciences of the United States of America. 2011;108(37):15414-9. Epub 2011/08/10. doi:
496 10.1073/pnas.1110854108. PubMed PMID: 21825165; PubMed Central PMCID: PMCPmc3174680.
497 31. Koyuncu OO, Hogue IB, Enquist LW. Virus infections in the nervous system. Cell Host Microbe.
498 2013;13(4):379-93. doi: 10.1016/j.chom.2013.03.010. PubMed PMID: 23601101.
499 32. Kong FQ, Zhao SJ, Sun P, Liu H, Jie J, Xu T, et al. Macrophage MSR1 promotes the formation of foamy
500 macrophage and neuronal apoptosis after spinal cord injury. Journal of neuroinflammation. 2020;17(1):62.
501 Epub 2020/02/19. doi: 10.1186/s12974-020-01735-2. PubMed PMID: 32066456; PubMed Central PMCID:
502 PMCPmc7027125.
503 33. Felt SA, Grdzelishvili VZ. Recent advances in vesicular stomatitis virus-based oncolytic virotherapy: a
504 5-year update. J Gen Virol. 2017;98(12):2895-911. doi: 10.1099/jgv.0.000980. PubMed PMID: 29143726.
505 34. Liang M, Yan M, Lu Y, Chen IS. Retargeting vesicular stomatitis virus glycoprotein pseudotyped lentiviral
506 vectors with enhanced stability by in situ synthesized polymer shell. Human gene therapy methods.
507 2013;24(1):11-8. Epub 2013/01/19. doi: 10.1089/hgtb.2012.113. PubMed PMID: 23327104; PubMed Central
508 PMCID: PMCPmc4275776.
509 35. Lin K, Zhong X, Ying M, Li L, Tao S, Zhu X, et al. A mutant vesicular stomatitis virus with reduced
510 cytotoxicity and enhanced anterograde trans-synaptic efficiency. Molecular brain. 2020;13(1):45. Epub
511 2020/03/22. doi: 10.1186/s13041-020-00588-3. PubMed PMID: 32197632; PubMed Central PMCID:
512 PMCPmc7085170.
513 36. You F, Wang P, Yang L, Yang G, Zhao YO, Qian F, et al. ELF4 is critical for induction of type I interferon and
514 the host antiviral response. Nature immunology. 2013;14(12):1237-46. Epub 2013/11/05. doi: 10.1038/ni.2756.
515 PubMed PMID: 24185615; PubMed Central PMCID: PMCPmc3939855.
516 37. Beaudoin GM, 3rd, Lee SH, Singh D, Yuan Y, Ng YG, Reichardt LF, et al. Culturing pyramidal neurons from
517 the early postnatal mouse hippocampus and cortex. Nature protocols. 2012;7(9):1741-54. Epub 2012/09/01.
518 doi: 10.1038/nprot.2012.099. PubMed PMID: 22936216.
519 38. Yardeni T, Eckhaus M, Morris HD, Huizing M, Hoogstraten-Miller S. Retro-orbital injections in mice. Lab
520 Anim (NY). 2011;40(5):155-60. doi: 10.1038/laban0511-155. PubMed PMID: 21508954.
521 39. Wang P. Exploration of West Nile Virus Infection in Mouse Models. Methods Mol Biol. 2016;1435:71-81.
522 doi: 10.1007/978-1-4939-3670-0_7. PubMed PMID: 27188551.
523
524
525
526

527 **Figure legends**

528 **Fig. 1 Msr1 contributes to VSV pathogenesis in mice**. **a)** *Msr1* mRNA expression in
529 various tissues of wild-type (WT, C57BL/6) and *Msr1*$^{-/-}$ mice, N=3 mice per genotype. **b)**
530 The survival curves and disease scores of WT and *Msr1*$^{-/-}$ mice challenged with $1\times10^7$
531 plaque-forming units (PFU) per mouse of VSV by retro-orbital injection, N=12
532 mice/genotype. $P$=0.001 (log-rank test), * $P$<0.05; ** $P$<0.01; *** $P$<0.001; **** $P$<0.0001,
533 non-parametric Mann-Whitney U test. **c)** The WT mice with paralyzed hind-limbs at day 6
534 post infection. **d)** Immunoblots of Msr1 protein expression in macrophages of WT, *Msr1*$^{-/-}$
535 and *Msr1*$^{-/+}$ littermates. Beta Actin (Actb) is a housekeeping control. **e)** The survival curves
536 and disease scores of *Msr1*$^{-/-}$ and *Msr1*$^{-/+}$ littermates challenged with $1\times10^7$ PFU/mouse of
537 VSV by retro-orbital injection, N=6 mice/genotype. All the error bars: mean ± S.E.M.

538

539 **Fig. 2 Msr1 is dispensable for systemic VSV dissemination and innate immune**
540 **responses**. **a)** The viremia of WT mice, *Msr1*$^{+/-}$ and *Msr1*$^{-/-}$ littermates infected with VSV,
541 assessed by quantitative RT-PCR, N=6 mice/genotype. **b)** The serum levels of type I IFN and
542 inflammatory cytokines in *Msr1*$^{+/-}$ and *Msr1*$^{-/-}$ littermates after VSV infection, assessed by
543 multiplex ELISA, N=6 mice/genotype. All the data are presented as mean ± S.E.M. and
544 statistical significance are analyzed by non-parametric Mann-Whitney U test.

545

546 **Fig. 3 Msr1 is critical for VSV infection specifically in the spinal cord**. Quantitative
547 RT-PCR analyses of VSV loads in **a)** different tissues of *Msr1*$^{+/-}$ mice (N=3 mice per group),
548 **b)** the spinal cords and **c)** the brains of *Msr1*$^{+/-}$ and *Msr1*$^{-/-}$ littermates on day 6 after infection

549 (N=6 mice/genotype). **d)** The VSV titers in the spinal cord and brain of *Msr1*$^{+/-}$ and *Msr1*$^{-/-}$
550 littermates on day 6 after infection, as assessed by plaque forming assay. N=6 mice/genotype.
551 **e)** Msr1 mRNA expression in different tissues of mock and VSV-infected mice on day 6 after
552 infection, N=3 mice per group. **f)** Correlation between *Msr1* expression and VSV load in
553 various tissues after VSV infection, N=3 mice per group. The mRNA expression of Class A
554 and B scavenger receptors in **g)** the spinal cord and **h)** the brain on day 6 after VSV infection,
555 as assessed by quantitative RT-PCR, N=3 mice per group. **i)** *Ldlr* mRNA expression in the
556 brain and spinal cord, N=3 mice per group. Mock: no virus. All the data are presented as
557 mean ± S.E.M. and statistical significances are analyzed by non-parametric Mann-Whitney U
558 test, * $P<0.05$, ** $P<0.01$.
559
560 **Fig. 4 Msr1 mediates cellular entry of VSV in primary mouse cells**. VSV loads in primary
561 neurons of *Msr1*$^{+/-}$ and *Msr1*$^{-/-}$ littermates at 36 h after inoculation (multiplicity of infection
562 =3), as assessed by **a)** quantitative RT-PCR and **b)** plaque forming assay. Each dot represents
563 an individual mouse. **c)** Immunoblots of Msr1 protein expression in WT and *Msr1*$^{-/-}$ bone
564 marrow-derived macrophages (BMDM) and peritoneal macrophages (PM). **d)** VSV-G
565 protein expression in BMDM, **e)** virus titer in culture medium and **f)** VSV-GFP fluorescence
566 under microscopy in BMDM at 48 h after VSV infection, N=3 biological replicates.
567 Objective: 20x, Scale bar: 100 μm. **g)** Quantitative RT-PCR analyses of VSV virions attached
568 to BMDM (4℃ for 2 h) and entry into BMDM (37℃ for 30 min), N=3 biological replicates.
569 Beta Actin (Actb) is a housekeeping control. Mock: no virus. All the data are presented as
570 mean ± S.E.M. and statistical significances are analyzed by a standard two-tailed unpaired

571 Student's t-test, * $P<0.05$, ** $P<0.01$.

572

573 **Fig. 5 MSR1 facilitates cellular entry of VSV through its extracellular domain**. **a)**
574 Immunoblots of VSV-G protein level, **b)** VSV-GFP fluorescence intensity and **c)** VSV titers
575 in the cell culture medium of WT and *MSR1*$^{-/-}$ trophoblasts at 12 h after VSV infection
576 (MOI=0.5). N=3 biological replicates. **d)** MSR1 protein expression, VSV-G protein level, **e)**
577 VSV-GFP fluorescence intensity and **f)** VSV titers in the culture medium of WT and
578 MSR1-overexpressed trophoblasts at 12 h after VSV infection (MOI=0.5). N=3 biological
579 replicates. The VSV-GFP fluorescence intensity in **b)** and **e)** was calculated from 9 random
580 fields of view from three biological replicates. Objective: 4x (top) and 20x, Scale bar: 100
581 μm. **g)** Immunoblots of VSV-G protein level in *MSR1*$^{-/-}$ trophoblasts with epichromosomal
582 complementation of an empty vector or FLAG-MSR1 expression plasmid at 12 h after VSV
583 infection, MOI=0.5. **h)** The protein expression of different FLAG-tagged MSR1 fragments at
584 24 h after transfection of plasmids in trophoblasts. IB: immunoblotting. Amino residues 1-50
585 (cytoplasmic N-tail), 1-80 (cytoplasmic N-tail plus transmembrane), 51-end (extracellular
586 domains with transmembrane), and 1-end (full-length). **i)** VSV-G protein level and **j)**
587 VSV-GFP fluorescence intensity in the trophoblasts overexpressing FLAG-MSR1 fragments
588 at 12 h after VSV-GFP infection, MOI=0.5, N=3 biological replicates. Beta Actin (ACTB) is
589 a housekeeping control. Mock: no virus. All the data are presented as mean ± S.E.M. and
590 statistical significances are analyzed by a standard two-tailed unpaired Student's t-test, **
591 $P<0.01$, *** $P<0.001$, **** $P<0.0001$.

592

593 **Fig. 6 MSR1 interacts with VSV glycoprotein G via its extracellular domains**. **a-c)**
594 Binding of MSR1 to VSV virions. FLAG-MSR1 (human, 1-end) and its fragments (aa1-80,
595 51-end) were expressed in HEK293 cells and immunoprecipitated (IP) using anti-FLAG
596 antibody-coated magnetic beads, which were then incubated with intact VSV-GFP virions (4℃
597 for 2 h). The bound virions were eluted for **a)** immunoblotting (IB) with a mouse monoclonal
598 anti-FLAG and rabbit anti-VSV-G antibody, **b-c**) for re-infection in Vero cells for 12 h
599 followed by detection of **b)** VSV-GFP by fluorescence microscopy and **c)** VSV-G protein
600 level by immunoblotting. Mock: no virion. **d)** co-IP of FLAG-MSR1 and its fragments with
601 VSV-G in HEK293 cells transfected with expression plasmids. WCL: whole cell lysate.
602 Arrows point to the faint protein bands.

603
604
605
606
607
608
609
610
611
612
613
614
615
616
617
618
619
620
621

Fig.1

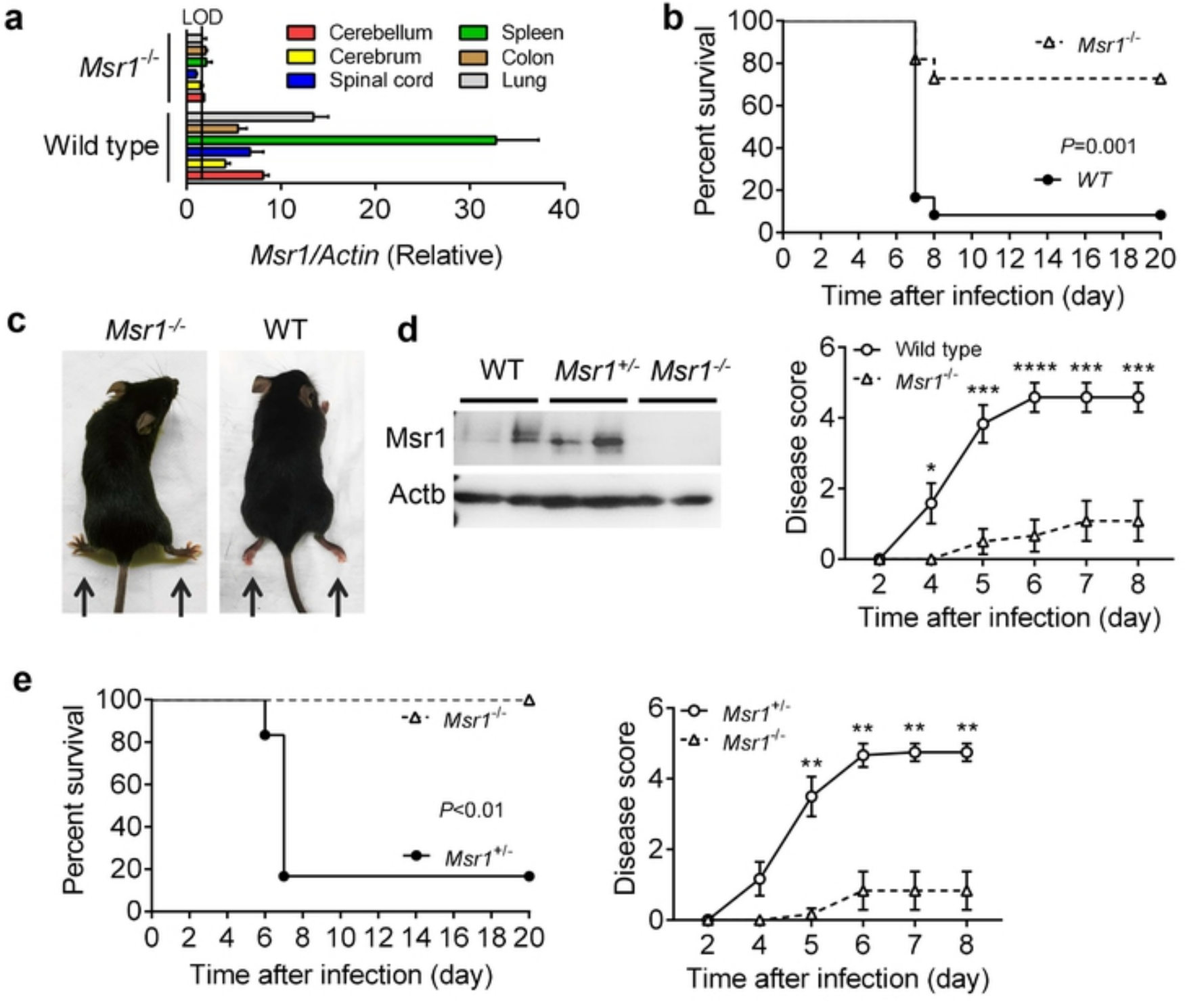


Figure1

Fig.2

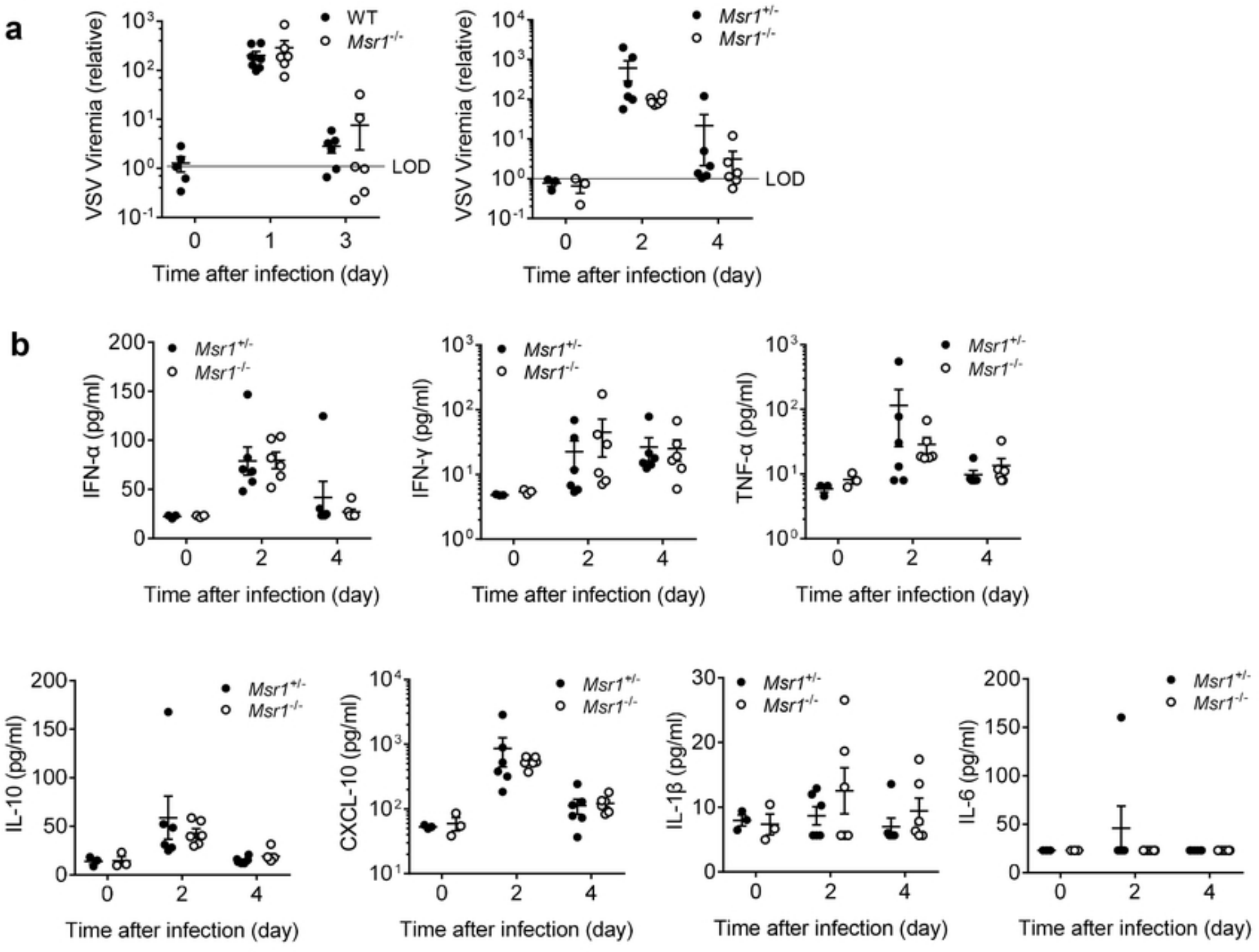


Figure2

Fig.3

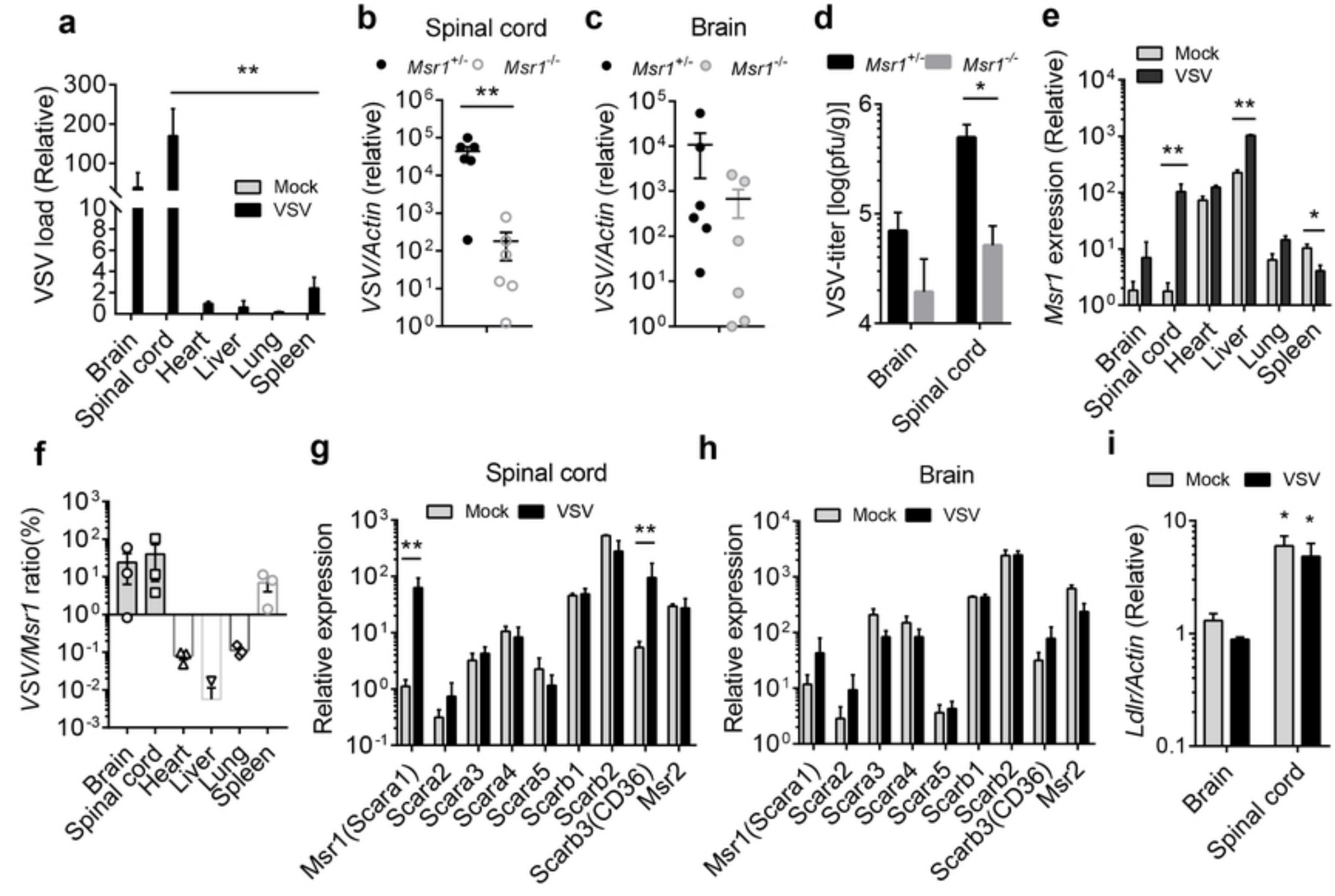


Figure3

Fig.4

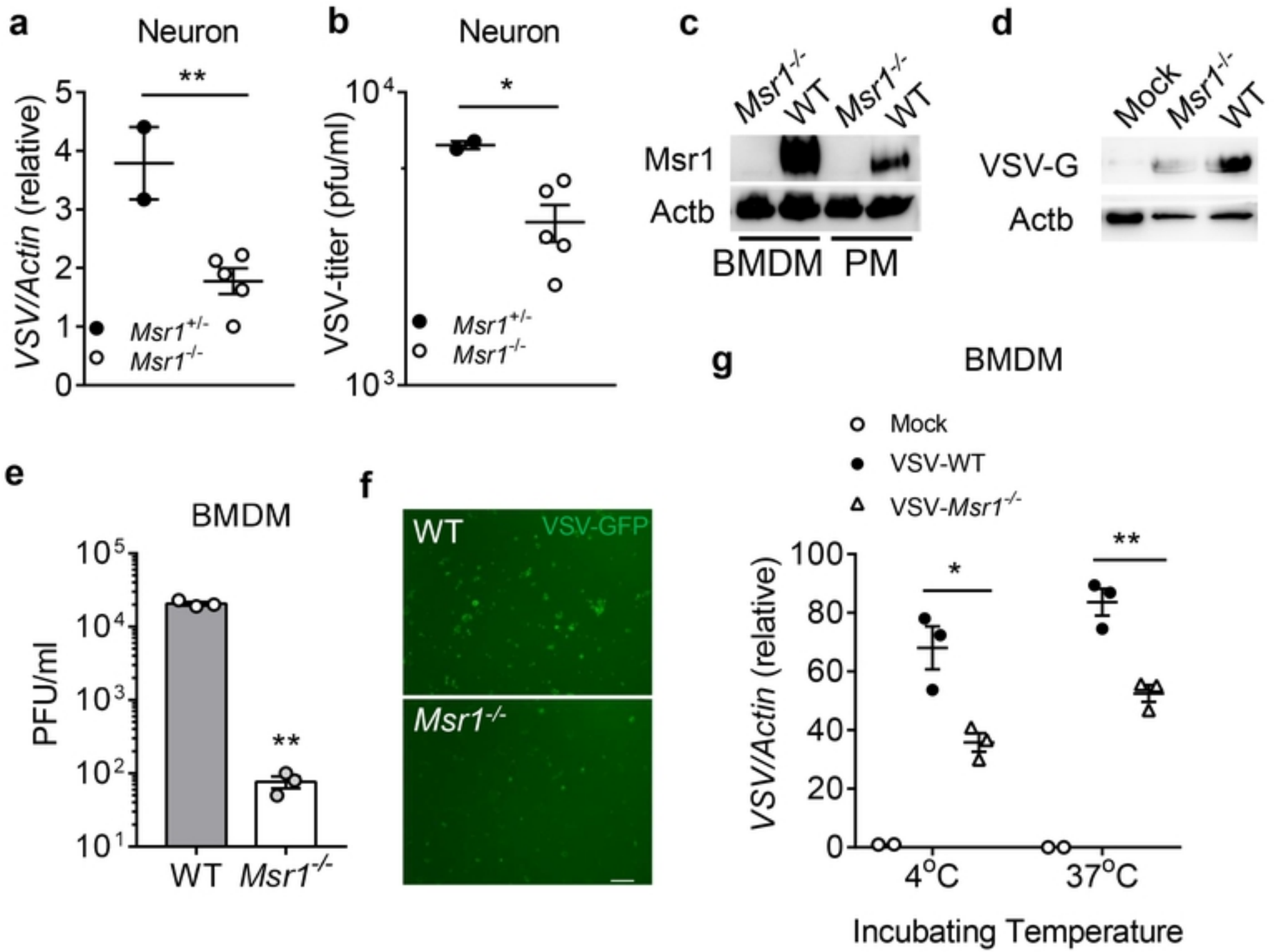


Figure4

Fig.5

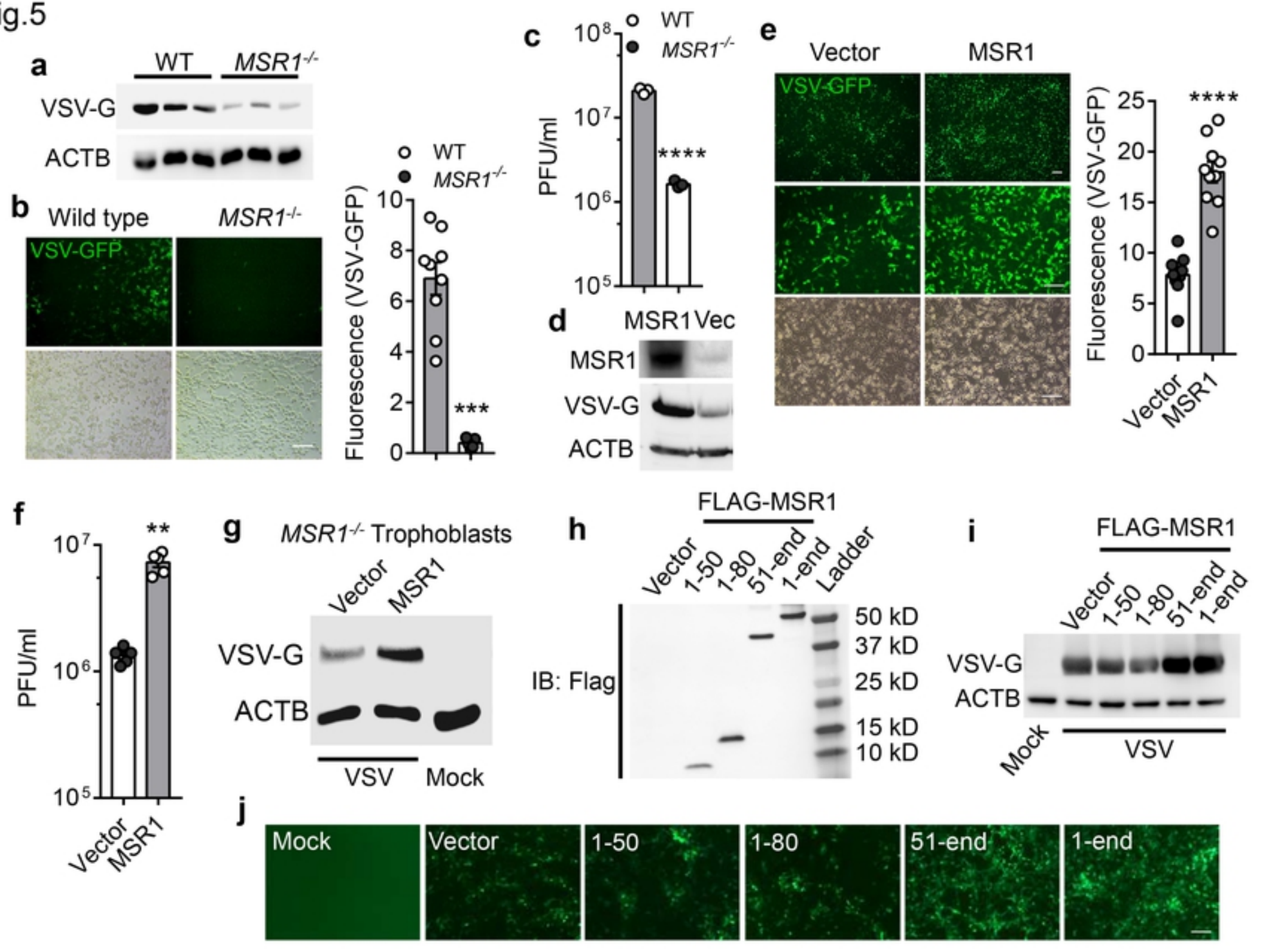


Figure5

Fig.6

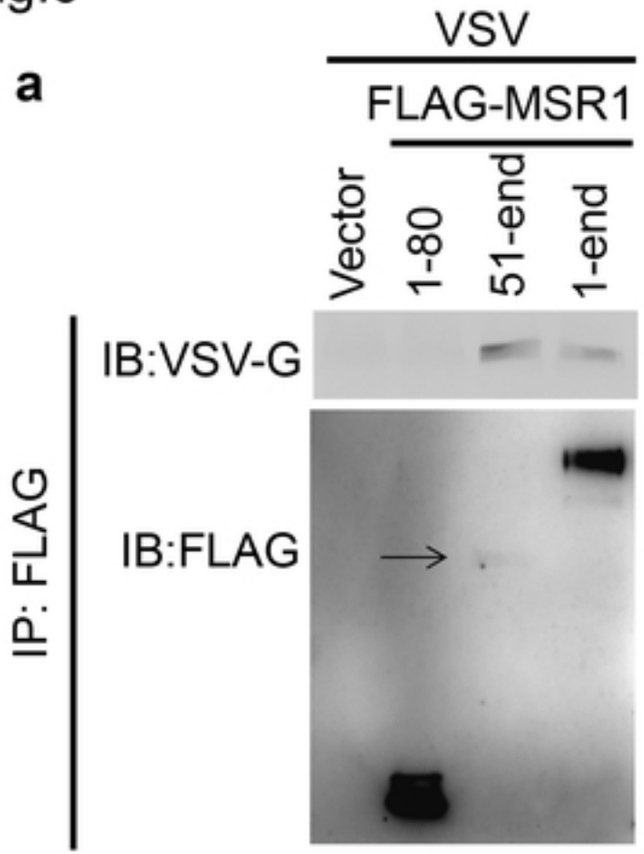


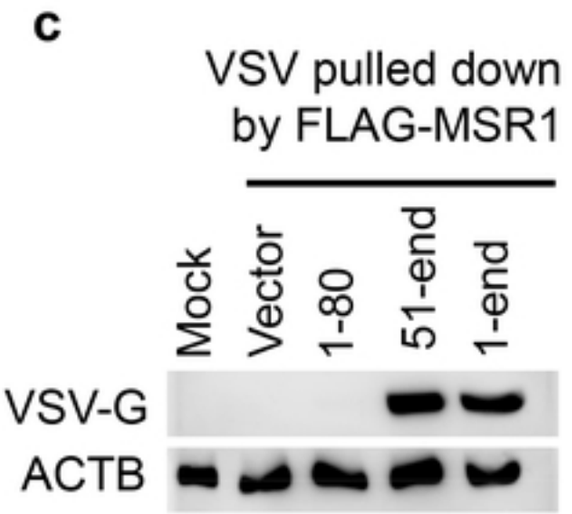


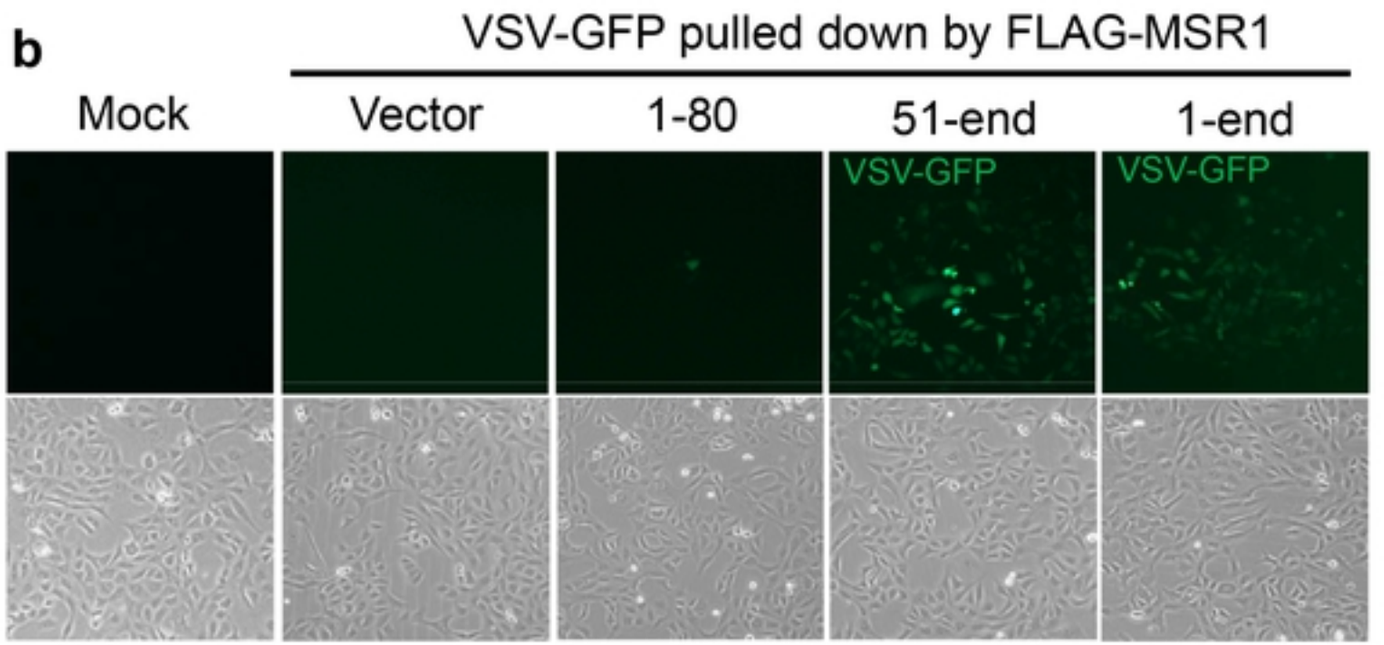


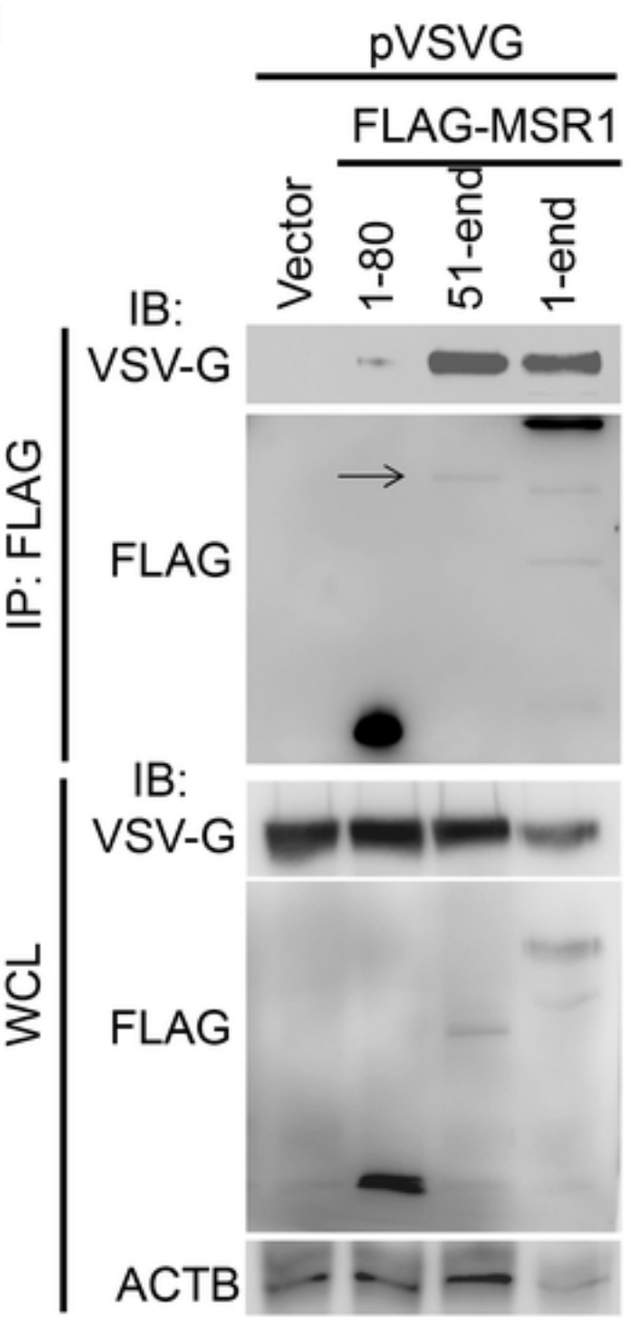


Figure6